Exotic applications of muons: from fusion to the life sciences

K Nagamine

KEK and RIKEN

1 Principles of muon catalysed fusion (μCF)

1.1 Introduction

Nuclear fusion is a phenomena of well-known nuclear reactions occurring among, mostly, light nuclei when they come close to each other within a few femtometres, the range of the nuclear interaction. (1fm = 10^{-13}cm). There, because of a reduction of the sum of the rest masses from the initial state to the final state, one can expect the production of energy. In Table 1, the typical fusion reactions among light nuclei are summarised.

p+d $\rightarrow$ ^{3}He + γ	5.5 MeV
p+t $\rightarrow$ ^{4}He +γ	19.8 MeV
d+d $\rightarrow$ ^{3}He +n	3.3 MeV
$\rightarrow$ t+p	4.0 MeV
$\rightarrow$ ^{4}He +γ	24.0 MeV
d+t $\rightarrow$ ^{4}He +n	17.6 MeV
t+t $\rightarrow$ ^{4}He +2n	10.0 MeV
d+ ^{3}He $\rightarrow$ ^{4}He + p	18.35 MeV

Table 1. *Typical fusion reactions*

Most fusion reactions have been studied at high energy (above 100keV) using accelerators. In this case the reaction partners must come close enough together to overcome the Coulomb repulsion. As described in this article, the muon catalysed fusion (frequently the word of μCF is used hereafter) phenomenon is a nuclear reaction at zero energy. Thus we must interpolate our knowledge of the nuclear physics of the fusion reaction at high energy.

Among two types of muons, namely, μ^+ and μ^-, only the μ^- is involved in muon catalysed fusion research. The most fascinating features regarding muon catalysed fu-

sion concern (1) types of phenomena related to the interplay of nuclear phenomena and atomic phenomena related to the interplay of nuclear and electromagnetic interactions, respectively, and (2) possible future applications to energy resources. This is particularly true regarding the μCF in a deuterium and tritium (DT) mixture with a high density ϕ comparable to the liquid hydrogen density, ϕ_0 (0.425×10^{23} nuclei/cc). In the following, the present understanding and future prospects of the μCF are summarised with a particular emphasis on the DT μCF and some limited descriptions on the μCF in the other systems listed in Table 1.

1.2 Muonic atoms and molecules

After the end of slowing down inside the condensed matter, the accelerator producing MeV-μ^- takes the form of muonic atoms. Then, in a cascade process inside the atom, the μ^- reached to the ground-state of muonic atom where the μ^- stays until it decays into electron or until it is captured to the nucleus.

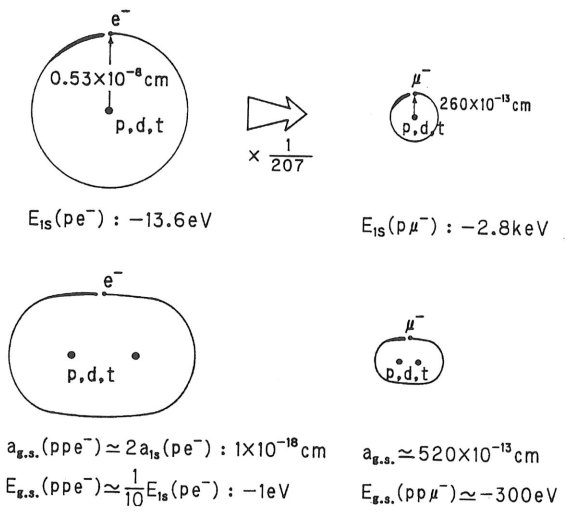

Figure 1. *Properties of muonic hydrogen atom and muonic hydrogen molecular ion.*

The properties of the ground-state of muonic atoms where the μ^- stays most of its lifetime after being injected into the materials are characterised by the following factors; the binding energy, size, lifetime, etc. Based upon the Bohr model of hydrogen-like single-electron atom, as depicted in Figure 1, the radial wavefunction $R_\mu(1s)$ and binding energy $E_\mu(1s)$ of the ground-state can be described as follows, when the μ^- forms a muonic atom around the light nuclei with atomic number Z.

$$R_\mu(1s) \approx \frac{270}{Z} \times 10^{-13} \quad \text{(cm)}$$
$$E_\mu(1s) \approx 13.6 \times 207 \times Z^2 \quad \text{(eV)}$$

This is almost correct until the 1s orbital becomes close to the nuclear size, which increases as $1.2 \times A^{1/3} \times 10^{-13}$(cm) where A is the mass number of the nucleus. Therefore, correction

becomes significant for nuclei heavier than Fe, Cu, etc. The energy levels are significantly changed from the classical and point-nucleus approximation due to the following two corrections; finite-size nature of nuclear charge distribution and vacuum polarization.

The lifetime of the ground state is also subject to the nuclear capture rate λ_c which depends upon the Z number; the higher the Z of the nuclei, the more the nuclear capture rate is enhanced. The elementary nuclear capture process is μ^-+p$\rightarrow$n+ν_μ . Therefore, the capture rate is the μ^- density at nucleus proportional to $[1/R_\mu(1s)]^3$ (proportional to Z^3) times the proton number (proportional to Z) so that Λ_c is proportional to Z^4 (the Z^4 law). Thus, the nuclear capture rate is given as

$$\Lambda_c = \Lambda_0 Z^4$$

where Λ_0 is the capture rate to the hydrogen. Various theoretical and experimental studies have been carried out to obtain the further correction terms to the Z^4 law.

When the μ^- injected into materials composed of many different elements, the μ^- is captured to each atom according to specific population mechanism. This model of atomic capture was first studied by Fermi and Teller (1947). Sometime, the atomic capture itself is called Fermi-Teller law.

The original Fermi-Teller law suggests the following populations $P(Z_1)$, $P(Z_2)$, ... for the molecules made of elements like $(Z_1)_m(Z_2)_n \ldots$ (*e.g.* for Fe_2O_3 we have $Z_1 = 26$, $m = 2$, $Z_2 = 6$ and $n = 3$),

$$P(Z_1) = mZ_1, \qquad P(Z_2) = nZ_2, \ldots$$

Experimentally, several studies have been made to test the Fermi-Teller law. A systematic deviation was seen. Significant examples are found in the case of oxides like Z_kO_m, where the relative population $(m/k)(P(Z)/P(O))$ is found not to be $Z/8$ as the Fermi-Teller law predicted. Moreover, the deviation seems to follow the periodic table. Revised atomic capture law has been proposed by Ponomarev (1973), Daniel (1975), Leon (1977), Schneuwley (1977) and others.

Among hydrogen isotopes, p, d and t, the formation rate of each muonic atom is considered to be proportional to the concentration of each nuclei, no matter how nuclei are contained in specific molecular states.

As described later, the muon catalysed fusion takes place inside the muon molecular (more correctly a muonic molecular ion) formed by two nuclei such as d, t and the μ^-. Now, let us consider how small molecules can be formed. The μ^- at the ground state of muonic hydrogen is known to take an orbit with a radius of 270fm and a binding energy of 2.8keV. By analogy to the conversion from H(1s) to H_2^+ (g.s.), where the radius of H_2+ (g.s.) becomes 2 times larger and the binding energy becomes 1/10 times smaller than that of H(1s), respectively, one can consider the $(H_2\mu^-)^+$ molecular ion takes a radius of 2×270fm and a binding energy of $2.8\times(1/10)$ keV as shown in Figure 1.

1.3 Basic concepts of muon catalysed fusion

The basic phenomena of the μCF involve the following two processes; 1) the formation of a small molecule, called a muonic molecule, consisting of two nuclei and a μ^- and an intramolecular fusion reaction and 2) a series of chain reactions of the fusion reactions mediated

by a single μ^-. Regarding the case of the DT μCF, these two processes are schematically summarised in Figures 2 and Figure 3. Sometimes, historically in particular, the chain reaction is presented in the form of a cyclic reaction by connecting the final part of one unit of the chain reaction to the beginning, as shown in Figure 4. The basic processes for DT μ CF, the details of which are described in Section 2, can be summarised as follows.

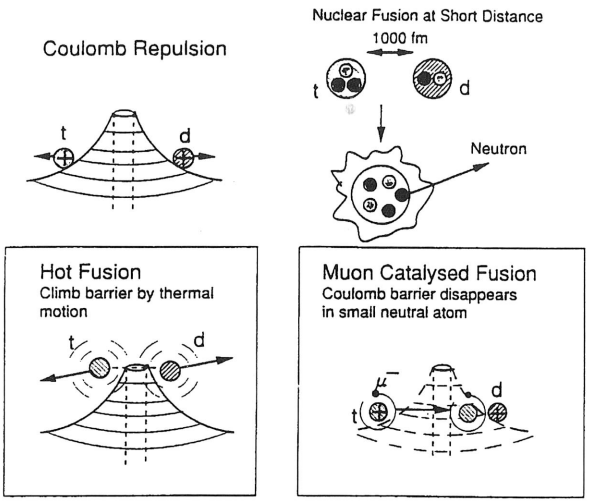

Figure 2. *Conceptual view of the role of a negative muon used to remove the repulsive potential between d and t to catalyze nuclear fusion with reference to thermal nuclear fusion.*

After high-energy μ^- injection and stopping in a DT mixture, either the (dμ) or (tμ) atom is formed, depending upon the concentrations of D and T, C_d and C_t respectively with $C_d + C_t = 1$. Because of the difference in the binding energy of atomic states (either excited or ground) between (dμ) and (tμ), the μ^- in the atomic state of (dμ) takes a transfer reaction to (tμ) during a collision with the surrounding t in either DT or T_2 molecule like (dμ) + t $\rightarrow$ (tμ) + d at the rate of λ_{dt}. The thus formed (tμ), either after thermalization or before, does react with D_2, DT or T_2 to form a muon molecule, where the formation of a specific state of the (dtμ) molecule through the resonant formation mechanism is important at a rate of $\lambda_{dt\mu}$. Once the (dtμ) molecule is formed at the specific state, a rapid cascade transition process of the μ^- inside the dtμ molecule takes place followed by the fusion reaction at the low-lying molecular state of the (dtμ), where a distance between d and t is close enough for the fusion reaction to take place. Then, a 14-MeV neutron and 3.6-MeV α are emitted. After the fusion reaction inside the (dtμ) molecule, most of the μ^- is liberated to participate into the second μCF cycle. Some small fraction of the μ^- has a possibility to be captured by the recoiling positively charged α. The probability of forming an $(\alpha\mu)^+$ ion is called the sticking probability ω_s. Once the $(\alpha\mu)^+$ is formed, since the μ^- has an initial kinetic energy of 90keV compared to the 10keV binding energy of the ground state of ($\alpha\mu$), the μ^- can be stripped from the stuck ($\alpha\mu$) ion. This process is called regeneration. Thus, μ^- in the form of either a non-stuck μ^- or a regenerated one from the stuck ($\alpha\mu$) can participate into the second μCF cycle.

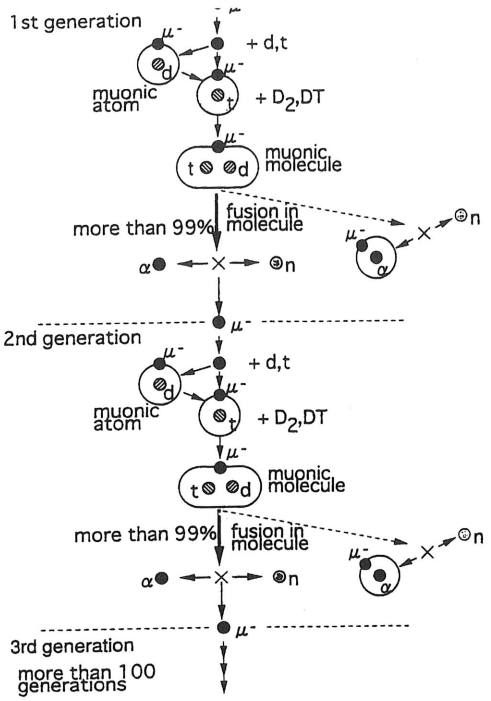

Figure 3. *Chain reaction of the muon catalysed fusion phenomena in a DT mixture.*

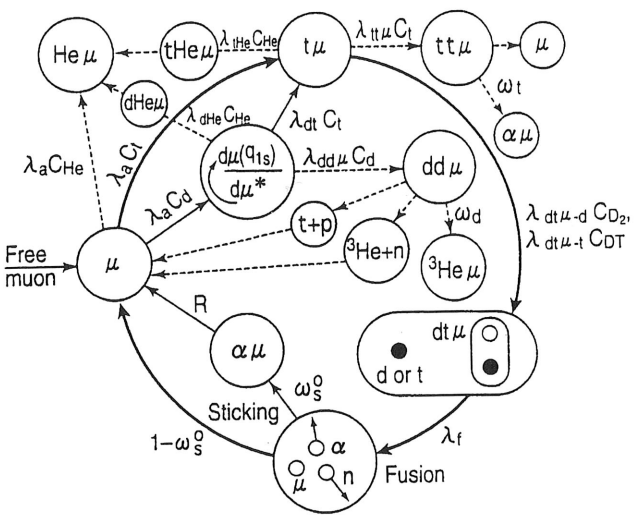

Figure 4. *Cyclic reaction representation of the chain reaction of the muon catalysed fusion phenomenon in a DT mixture, including the hyperfine effect and possible loss processes other than (aμ) sticking.*

Some details concerning the dtμ μCF cycle are shown in Figure 4. In the (dμ) to t transfer, there is a possibility that the μ^- is transferred from excited (dμ) states. Since t, d and μ^- have spin, there should be a hyperfine (spin-dependent) effect in the formation process of a muon molecule. Also, the existence of He impurity is inevitable due to t-decay and μCF itself; the μ^- loss due to capture to a ^{3}He must be taken into account.

In fact, various types of physical processes are involved in these main processes. The fusion reaction in a small muon molecule is the most significant part where nuclear interaction dominates. Also, a nuclear interaction does affect muon sticking and related processes. Thus the remaining processes are due mainly to electromagnetic-interactions. There, in order to understand electromagnetic-interaction related μCF phenomena, the basic roles of the μ^- can be understood by considering the μ^- to be a heavy electron with a mass ratio m_μ/m_e of 207.

Therefore, in order to understand the physics of the μCF, the following classification of the processes is relevant: (1) nuclear-process fusion reaction in a muon molecule; (2) intermediate-process muon sticking regeneration and electromagnetic; (3) atomic and molecular processes, muonic atom formation/ intra-atomic cascade and slowing-down, muon transfer among hydrogen isotopes, formation of a muon molecule/intra-molecular transition and a He impurity effect in the μCF of hydrogen isotopes, etc.

The concept of the μCF has been introduced independently by Frank (1947) and Sakhalov (1948). An experimental observation of pdμ μCF was made by Alvarez et al (1956) at Berkeley. The major historical trend of the μCF studies is summarised in Table 2. Several review articles are available regarding the μCF phenomena (Breunlich 1989, Ponomorev 1990, Nagamine and Kamimura 1998).

1947	Hypothesis of the μCF cycle	Frank
1948	Estimate of the fusion rate λ_f^{dd}, λ_f^{dt}	Sakharov
1956	Observation of pdμ fusion	Alvarez
1957	Calculation of the dtμ cycle and sticking	Jackson
1966	Observation of the T-dependence of $\lambda_{dd\mu}$	Dzhelepov
1967	Theory of the resonant formation of ddμ	Vesman
1977	Prediction of large $\lambda_{dt\mu}$	Gerstein, Ponomarev
1979	Observation of the upper limit on $\lambda_{dt\mu}$	
1979	Observation of the hyperfine effect in $\lambda_{dd\mu}$	PSI
1982	Measurement of $\lambda_{dt\mu}$, λ_{dt}	LAMPF
1987	Observation of X-rays from $\mu\alpha^+$ in DT μCF	PSI, KEK
1987	Observation of X-rays from dHeμ	KEK
1993	Observation of a large $\lambda_{dd\mu}$ in solid D_2	TRIUMF
1994	Observation of X-rays from muon tranfer	PSI, KEK
1995	Observation of $\lambda_{dt\mu}$ with eV tμ	TRIUMP
1997	Systematic studies of X-rays, neutrons from DT μCF	RIKEN-RAL

Table 2. *Major historical trends of muon catalysed fusion studies*

2 Present and future of muon catalysed fusion

2.1 Present understandings

Nuclear fusion reaction inside the muon molecule

In the concept of the μCF, the fusion reaction becomes realised by utilizing a neutral small atom formed by the μ^- and hydrogen isotopes and by forming a small molecule (actually molecular ion) among the d, t and μ^- for the DT μCF. Since the range of the nuclear interaction (a few fm) is close to the size of the molecule, with the help of zero-point motion of the molecular ion, the fusion reaction proceeds at a high rate.

Historically, the rate of nuclear fusion inside the small muon molecule ($\lambda_{\rm fus}$) was calculated by the so-called factorization relations (Jackson 1957).

$$\lambda_{\rm fus} = a_{\rm fus}|\psi(R)|^2,$$

where $a_{\rm fus}$ is a reaction constant related to the fusion cross section at zero relative energy, which can be obtained by an interpolation from the nuclear reaction data at higher energies, and $|\psi(R)|^2$ is the probability density of finding the two nuclei at a distance of R. The constant $a_{\rm fus}$ can be obtained by the interpolation ($v \to 0$) with a description of the low-energy cross section of the fusion reaction,

$$\sigma = a_{\rm fus}\, c_0^2\, v,$$

where c_0 is the Gamov factor of s-wave scattering and v is the relative velocity at infinity. $\lambda_{\rm fus} \sim 10^{12}{\rm s}^{-1}$ was given.

There have been several shortcomings in factorization treatments of the fusion rate. First of all, we need knowledge concerning the fusion rate at the excited state of the muonic molecule specified by the rotational quantum number (J) and vibrational one (ν), since, as described later, the formation of a muonic molecule takes place at the excited state of the muon molecule. Secondly, distortion of the molecular wave function due to the nuclear interaction should be taken into account. Moreover, a correction is needed in the formula of $\lambda_{\rm fus}$ due to the dominance of a near-threshold resonance in the reaction cross section.

Advanced calculations of the fusion rates in the muonic molecule dtμ were made by Bogdanova *et al.* (1988) and Kamimura (1989) within the complex nuclear potential (optical potential) method and by Struensee *et al.* (1988) and Szalewicz *et al.* (1990/91)within the R-matrix method. Four types of calculations gave similar results concerning the fusion rates of the $J = 0$ states of (dtμ).

In order to understand the overall fusion rate in a muon molecule, the details concerning the intra-molecular cascade transitions should be known. As described later, the formation of a muonic molecule is done mostly via resonance reactions to form an excited rotational vibrational ($J\nu$) state with $J = \nu = 1$, which is very weakly bound with respect to the $(t\mu)_{1s}$ +d threshold. The de-excitation of the muonic molecule levels proceeds via Auger transitions, like

$$[(dt\mu)_{J\nu}d2e]^* \to [(dt\mu)_{J'\nu'}d2e]^* + e.$$

These Auger de-excitation processes of the muonic molecule have been theoretically estimated by Bogdanova *et al.* (1982). The essential parts of the results are summarised in Figure 5. The μ^- cascades down to the lower levels where the fusion reaction takes place. In Figure 5, the fusion reaction rates and the cascade transition rates for the DT μCF are summarised; 80% of the fusion takes place at the $(J\nu)$=(01) state and 20% at the (00) state, both of which are formed after cascading down from the (11) state. As also shown in Figure 5, in the case of ddμ , which is formed at the $(J\nu)$=(11) state, the fusion reaction takes place at the (11) and (10) state at a rate of 5×10^{12}s^{-1}. Combining all of these arguments on the rates of fusion and de-excitation, we can conclude that in a time of 10^{-11}s (rate of 10^{11}s^{-1}) the fusion reaction is completed in the muon molecule after the formation of the (11) state or after the formation of the dtμ molecule during a collision between (tμ) and D_2.

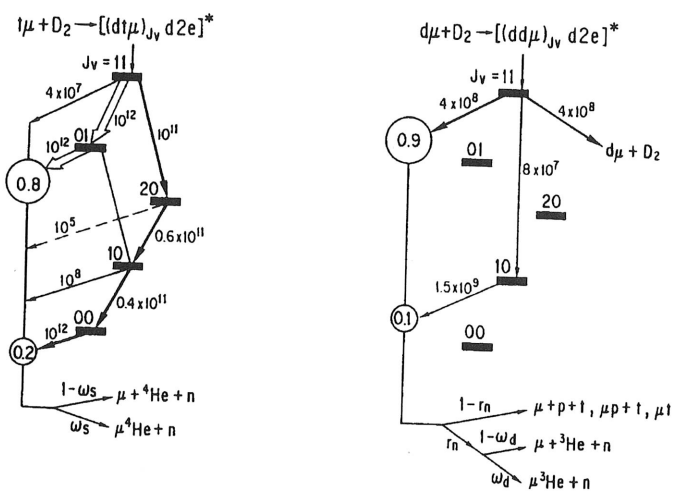

Figure 5. *Scheme of cascade processes in dtm and ddm molecleles after the resonant molecular formation at (1,1) state, calculated by Bogdanova et al.*

Muon sticking after nuclear fusion

So far, various experimental methods have been applied in order to investigate the muon catalysed fusion (μCF) phenomena for DT μCF. Let us explain how to obtain the reaction rates such as $\lambda_{dt\mu}$ and λ_{dt}, as well as the loss probability, such as ω_s, experimentally. The measurements of 14-MeV fusion neutrons can be used to obtain the fusion neutron yield, the cycling rate of the μCF, etc, where the decay electron measurement is mostly used for normalization purposes. Measurements of the characteristic X-ray in the μCF can also provide very valuable insights concerning each process of the μCF. A time-dependent measurement of these fusion neutrons and characteristic X-rays from muonic atoms/molecules can reveal the time evolution of μCF phenomena. Combinations of these experimental methods may provide the most satisfactory information about each process of the μCF cycle. Most of the experiments on DT μCF conducted at Los Alamos (Jones 1983, Jones 1986) and PSI (Breunlich, 1987) around 1990 have focused on neutron

measurements; both systematic neutron and X-ray combined measurements were carried out for the first time rather recently at RIKEN-RAL.

Regarding the rate of cycling (λ_c) with a loss probability (W) including muon-to-alpha sticking phenomena, several experimental methods have been applied. Here, we summarise relations between the experimental observables and physical parameters in the μCF cycle.

We first consider **neutron methods**. Measurements of the absolute yield Y_n and disappearance rate λ_n give us the loss rate W_n seen by neutrons, thus providing some limiting factor on ω_s. The total yield Y_n is obtained by integrating $Y_n(t)$ over all time:

$$Y_n(t) = \phi\lambda_c e^{-\lambda_n t},$$

$$Y_n = \frac{\phi\lambda_c}{\lambda_n}$$

where

$$\lambda_n = \lambda_0 + \lambda_c W_n,$$

$$W_n = \omega_s + \text{other losses}.$$

Secondly we consider **X-ray methods**. X-ray measurements from $(\mu\alpha)^+$ ions gives knowledge directly about sticking phenomena. The combination between $Y_x(t)$ and $Y_n(t)$ gives a direct measure of ω_s.

$$\begin{aligned} Y_x(t) &= \phi\lambda_c\kappa\omega_s^0 e^{-\lambda_n} \\ Y_x &= \frac{\phi\lambda_c\kappa\omega_s^0}{\lambda_n} \\ \frac{Y_x}{Y_n} &= \kappa\omega_s^0, \end{aligned}$$

where the κ, given by the theory of atomic processes of $(\mu\alpha)^+$ ion and ω_s^0 is the initial sticking right after the fusion reaction in the muon molecule. Actually ω_s^0 is the sum of the initial sticking to each orbit of the $(\mu\alpha)^+$ ion,

$$\omega_s^0 = \sum_{nl} \omega_s^0(nl).$$

The ω_s which appears in the total loss probability W_n is obtained after correcting the regeneration factor R,

$$\omega_s = \omega_s^0(1 - R).$$

Again, since the regeneration process depends upon the initial state of the $(\mu\alpha)^+$ ion, the ω_s should be written as

$$\omega_s = \sum_{nl}[1 - R(nl)]\omega_s^0(nl).$$

The experiments so far conducted as well as the values so far obtained are summarised in Figure 6, where values of the effective sticking of ω_s are presented as a function of ϕ.

Theoretical studies on the α-sticking have been initiated by Jackson (1957), where a sudden approximation has been applied. The probability of a $(\mu\alpha)^+$ atom formation in an nl state is given by

$$\omega_s^0(nl) = \sum_m |F_{nlm}|^2,$$

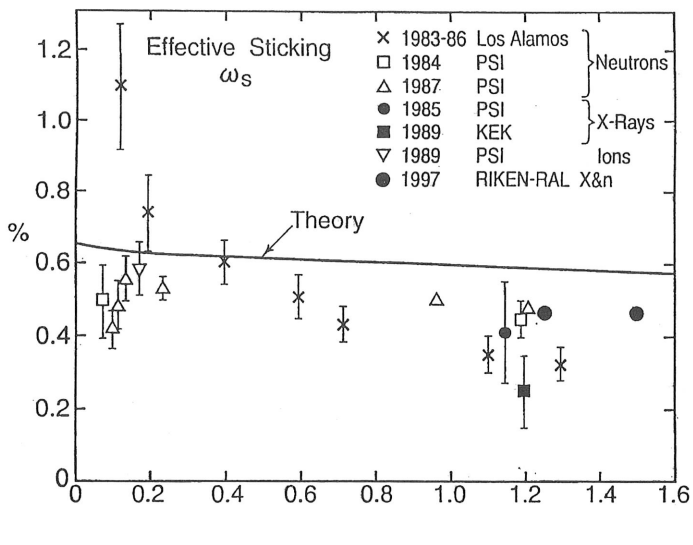

Figure 6. *The existing data concerning the sticking probability ω_s versus density ϕ in the muon catalysed fusion of a DT mixture*

where

$$F_{nlm} = \int \phi^*_{nml} e^{-i\mathbf{q}\cdot\mathbf{r}} \psi_0(\mathbf{r}) d^3\mathbf{r},$$

and ϕ_{nml} is the wave function of the $(\mu\alpha)^+$ atom in the state nlm. The vector $\mathbf{q}$ is equal to $m\mu\mathbf{v}$, where v is the velocity of $(\mu\alpha)^+$. The function $\psi_0(\mathbf{r})$ is the normalised muon wave function at the instant of fusion, which can be expressed through muon-molecule wave function, $\Psi_{J\nu}(\mathbf{r},\mathbf{R})$ by $\psi_0(\mathbf{r}) = N\psi_{J\nu}(\mathbf{r},\mathbf{R}=0)$, where $\mathbf{R}$ is the inter-nuclear distance and $\mathbf{r}$ is the muon coordinate with respect to the c.m. of the two nuclei, with N being the normalization constant.

Since 1986, X-ray measurements have been applied for the direct measurements of the $\mu-\alpha$ sticking probability in DT μCF at PSI (Bossy 1987), at UTMSL/KEK (Nagamine 1987, Nagamine 1990, Nagamine 1993) and recently at RIKEN/RAL. The experiment at PSI was performed with dc muons for a low C_t ($\sim 10^{-4}$) DT mixture, and that at KEK-MSL and RIKEN/RAL with pulsed muons for high-C_t (from 0.1 to 0.7). As for X-ray detection in dtμ μCF, the radiation background of the bremsstrahlung associated with t beta-decay is serious; the background, energy of which extends up to 17keV, does mask all ω_s-related X-rays (E(K_α)=8.2keV, E(K_β)=9.6keV, *etc.*). The use of pulsed muons, now available at KEK or at RIKEN/RAL, is really helpful; by operating the detection system only in a short time interval around a muon pulse, a significant improvement in the signal to noise ratio can be expected.

Following the first successful observation of Ka X-ray from $(\mu\alpha)^+$ in high density and high-C_t ($C_t = 0.3$) DT mixtures at UTMSL/KEK, systematic data on ω_s and λ_c have been obtained in high-density ($\phi = 1.2$–1.5) and high-C_t (C_t= 0.1–0.7) DT mixtures at RIKEN-RAL. There, several important improvements exist for the experimental method: (1) high intensity and low-background pulsed μ^- beam is used; (2) in order to obtain data for a ^{3}He-free pure DT mixture, in-situ ^{3}He removal as well as a chemical-analysis apparatus have been introduced. The actual steps for analyzing the data are taken as follows. (a) From the

time slope constant of the neutron yield Y_n, the value of $\lambda_c W_n = (\lambda_n - \lambda_0)/\phi$ is obtained, while, from the absolute neutron yield Y_n, the value of $\lambda_c = Y_n \lambda_n / \phi$ is obtained, so that both λ_c and W_n are obtained from the fusion neutron data. (b) After confirming the time slope constant of the X-ray yield $Y_x(t)$ being consistent with that of the fusion neutron λ_n, the value of $\kappa\omega_0$ is obtained by taking the ratio Y_x/Y_n so that the effective sticking seen by X-ray $\omega_s(\mathrm{X})(= Y_x/Y_n \times (1-R)/\kappa)$ is obtained by using the theoretical values of κ and R. (c) The overall consistency of this analysis can be checked by the condition $W_n \geq \omega_s$.

Slowing-down of hydrogen muonic atoms

All of the processes in μCF are started from the μ^- injection into a DT or D_2 mixture at high energies (MeV or higher). Then, the μ^- undergoes a slowing-down process by ionisation of the surrounding molecules/atoms and is eventually captured by the d or t to form a muonic d or t atom with a population proportional to the concentration.

It was pointed out both theoretically and experimentally that when a hydrogen-isotope target stays at liquid-hydrogen density ϕ_0, the time required for muonic atom formation is less than 10^{-12}s. The atomic state of the muonic atom is considered to take around $n = 14(m_\mu/m_e)^{1/2}$. The intra-atomic cascade transition then takes place via an Auger process at earlier stage (among higher atomic orbits) and radiative process at later stage, where a Stark-mixing process takes on a significant role at high target density. The cascade process to the ground-state of the muonic atom at $\phi = \phi_0$ is considered to take less than 10^{-11} s. The thus-formed neutral atoms undergo a further slowing-down process through a series of the elastic collisions with the surrounding atoms/molecules and eventually undergo the slowing-down towards thermalisation .

The above picture of muonic atom formation $\rightarrow$ intra-atomic cascade $\rightarrow$ thermalisation should be subject to a drastic change when the muonic hydrogen is formed in a high-density hydrogen-isotope mixture, e.g. a $(\mathrm{d}\mu)$ or $(\mathrm{t}\mu)$ atom in DT mixture. More rapid processes might be competing with either cascade or thermalisation processes. As described later, significant examples exist, such as muon transfer from an excited atomic state, muon-molecule formation at epithermal energy, etc. In any case, it had been recognised that we need more advanced knowledge concerning the most fundamental process of elastic scattering of a neutral hydrogen atom with the surrounding atoms and molecules.

Muon transfer among hydrogen isotopes

When the μ^- is injected into a DT mixture with D_2, T_2 and DT, the atomic states of $(\mathrm{d}\mu)$ and $(\mathrm{t}\mu)$ are produced roughly proportional to the concentration, C_d or C_t (with $C_d + C_t = 1$). In a DT mixture with a density ϕ of around ϕ_0, after injection with MeV energy, it takes 10^{-10}s for the μ^- to reach the ground state of either $(\mathrm{d}\mu)$ or $(\mathrm{t}\mu)$. Then, the μ^- remains during most of its lifetime in the ground-state, where the nuclear capture rate to either d or t is negligibly small ($400\mathrm{s}^{-1}$ for $\mathrm{d}\mu$). Since the ground-state energy of $(\mathrm{t}\mu)$ is deeper than that of $(\mathrm{d}\mu$) by 48eV, the μ^- at the ground state of $(\mathrm{d}\mu)$ can easily be transferred through the reaction $(\mathrm{d}\mu)$ + t $\rightarrow$ $(\mathrm{t}\mu)$ + d via a collision with t in either T_2 or DT. Theoretical studies on the ground-state transfer reaction among hydrogen isotopes have been carried out by several groups, and results of the transfer rate

at thermal energies ($\approx 2.7\times10^{8}\mathrm{s}^{-1}$) have explained the observed values.

Since the cascade transition rate of the μ^- in $(d\mu)$ or $(t\mu)$ is comparable to the radiative transition rate, there is a possibility for the μ^- to take a transfer reaction to $(t\mu)$ from its excited state of $(d\mu)$. By denoting q_{1s} to be a probability for the μ^- to reach to the ground state, the problem of the μ^- transfer at the excited state is sometimes called the q_{1s} problem; $q_{1s} = 1$ corresponds to the μ^- transfer after the μ^- reaches the ground state. Moreover, it has been pointed out that the $(d\mu) \rightarrow (t\mu)$ transfer reaction might occur at the epithermal energy of $(d\mu)$.

Some qualitative arguments can be summarised concerning the q_{1s} values at various C_t, ϕ and $E(d\mu)$, as shown in Figure 7. Some indirect knowledge existed about the values of q_{1s} in DT μCF based on C_t dependence measurements of fusion neutrons in a DT mixture. There is a deviation between theory and experiment. An example of a possible explanation may be the possible existence of the side-path proposed by Froelich and Wallenius (1995). The excited $(t\mu)_{2s}$ states formed via a transfer reaction from the excited $(d\mu)_{2s}$ states does collide with D_2 to resonantly form a $(dt\mu)^*$ molecule with $n = 2$, which mostly decays into the $(d\mu)_{1s}$ + t channel; apparently, $(d\mu)_{1s}$ is formed. This process can be considered as muon transfer from $(t\mu)_{2s}$ to $(d\mu)_{1s}$ via three-body resonances of $(dt\mu)$. This enlarges the $(d\mu)_{1s}$ population and improves the agreement with the experimental q_{1s}.

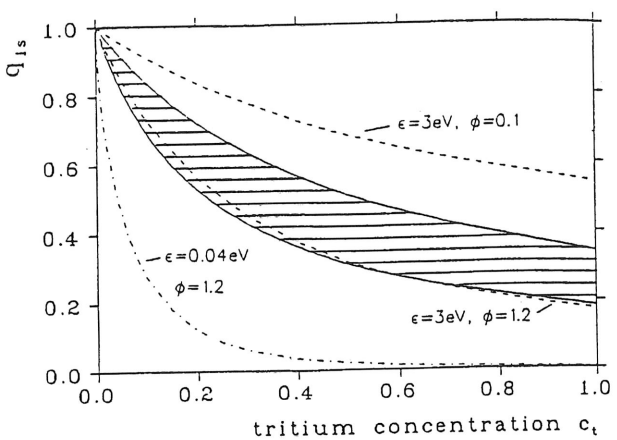

Figure 7. *Theoretical prediction of the q_{1s} values in the (dm) + t → (tm) + p transfer reaction and the experimental ones, extracted from neutron data in dtm-μCF as a function of CT at various (dm) energies and densities.*

Formation of the muon molecule

The lifetime of μ^- in vacuum and in a muonic hydrogen atom is 2.20μs, corresponding to a decay rate of $\lambda_0 = 0.455\times10^{6}\mathrm{s}^{-1}$. Due to the heavy mass, the atomic ground state of μ^- around d or t is small (260fm) and tightly bound (–2.7keV). A small neutral atom $(t\mu)$ may come close to d in D_2 or DT to form a small molecule of $(dt\mu)$+, whose ground state is small in size (520fm) and tightly bound (–300eV). Usually, the rate of formation of a

tightly bound molecular state is relatively slow. The most promising way is the so-called Auger capture, like

$$(d\mu) + D_2 \rightarrow [(dd\mu)de] + e^-,$$
$$(t\mu) + D_2 \rightarrow [(dt\mu)de] + e^-.$$

The theoretically predicted rate for the final state of a muonic molecule becomes fairly slow, such as $10^6 s^{-1}$ (comparable to λ_0).

However, Ponomarev and collaborators (Gerstein and Ponomarev 1977) have theoretically predicted that an extremely shallow bound state with both a rotational and vibration angular momentum of one $(J\nu) = (11)$ exists at an energy of $E_{11} = -0.6$eV, measured from the threshold energy of $(t\mu)_{1s}$ + d. Due to the existence of this shallow bound state, substantially enhanced formation rates are expected by the following reaction process called resonant molecular formations, as can be seen in Figure 8:

$$(t\mu) + D_2 \rightarrow [(dt\mu)_{11} d2e]^* \qquad (\lambda_{dt\mu-d}),$$
$$(t\mu) + DT \rightarrow [(dt\mu)_{11} t2e]^* \qquad (\lambda_{dt\mu-t}).$$

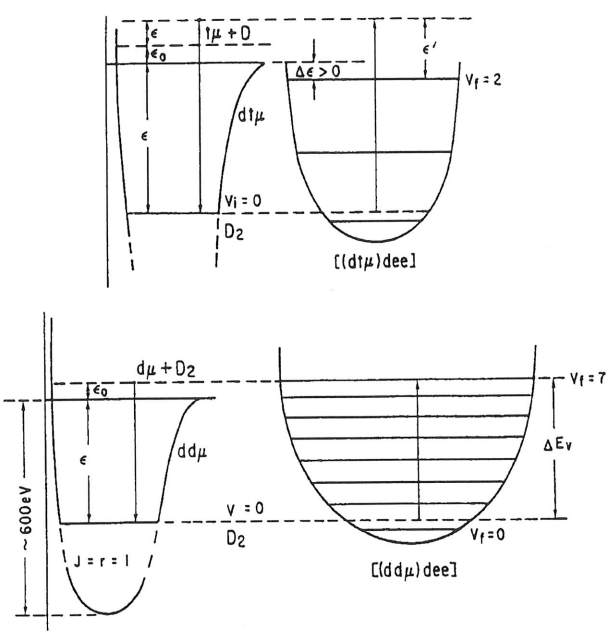

Figure 8. *Energy-level diagram for resonant molecular formation; $dt\mu$ versus $dd\mu$*

Experimentally, the formation rate of a muon molecule can be obtained through the relations between the observed cycling rate λ_c and the rate of the processes, *e.g.* λ_{dt} and $\lambda_{dt\mu}$. Let us consider high-density and high-C_t DT μCF and assume that the atomic capture rate ($\lambda_{d\mu}$ and $\lambda_{t\mu}$) and fusion rate ($\lambda_{\rm fus}$) are sufficiently high compared to the muon decay rate ($\lambda_{d\mu}$, $\lambda_{t\mu}$, $\lambda_{\rm fus} \gg \lambda_0$). Then, the cycle time (λ_c^{-1}) is due to the waiting time of dμ for muon transfer to t and that to form the molecule.

$$\frac{1}{\lambda_c} = \frac{q_{1s} C_d}{\lambda_{dt} C_t} + \frac{1}{\lambda_{dt\mu} C_d}.$$

Here, the factor $q_{1s}C_d$ is the probability that the muon reaches the ground state of $d\mu$, reflecting the fact that the transfer rate in the excited states of $(d\mu)$ are very rapid, as is the excited-state cascade.

In the above formula for λ_c, the maximum λ_c can be obtained for

$$C_t \approx (1+\gamma)^{-1}, \qquad \gamma = \sqrt{\lambda_{dt}/q_{1s}\lambda_{dt\mu}}.$$

In a DT mixture, there are three molecules D_2, DT and T_2 with the concentration ratios C_{D2}, C_{DT} and C_{T2}, respectively determined by the rate of chemical equilibrium. Thus, the rate $\lambda_{dt\mu}$ can be decomposed into the sum of two terms,

$$\lambda_{dt\mu} = \lambda_{dt\mu-d}C_{D2} + \lambda_{dt\mu-t}C_{DT}.$$

The idea of resonant molecular formation was experimentally confirmed, at least qualitatively, by the Dubna group in 1979, and in more detail by the experiments at Los Alamos (Jones 1983, Jones 1986) and at PSI (Breunlich 1987), where both "three-body effects" and a strange temperature dependence have been discovered . At the same time, a very rapid formation rate (order of $6\times10^8 s^{-1}$) was experimentally established for $\phi = \phi_0$ for a temperature range of up to 500K. These experimental data are summarised in Figure 9. Theoretical predictions based upon the resonant molecular formation have not been able

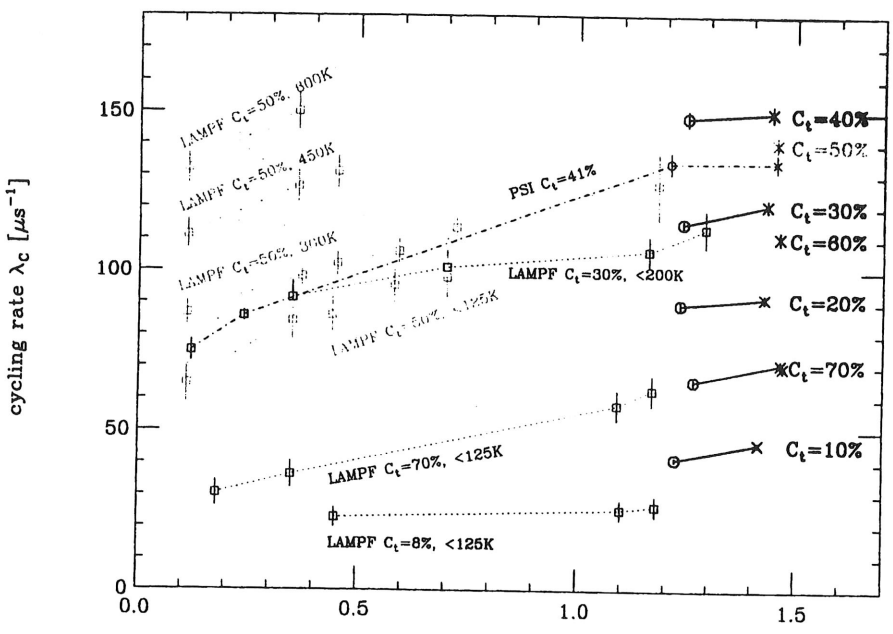

Figure 9. *Cycling rate of DT μCF versus density*

to explain the observed temperature dependence of the molecular-formation rate; according to theoretical predictions, there should be a steeper decrease in $\lambda_{dt\mu}$ towards the lowest temperature.

Experimentally, the existence of nonlinear many-body collisions in $\lambda_{dt\mu-d}$ has been consistently confirmed. There, the resonant process between $(t\mu)$ and D_2 proceeds under

the influence of the other D_2,

$$(t\mu) + D_2 + D_2 \rightarrow [(dt\mu)d2e]^* + D_2.$$

Experimental data have shown that such an effect does exist only for ($t\mu$) + D_2 and not for ($t\mu$) + DT. At the same time, the effect is effective only for $C_t \geq 0.3$. Assuming $\lambda_{dt\mu} = [\lambda^{(1)}_{dt\mu-d} + \lambda^{(2)}_{dt\mu-d}\phi]C_d + \lambda^{(1)}_{dt\mu-t}C_t$, from the Los Alamos experiment (Jones 1986), the following values are obtained; $\lambda^{(1)}_{dt\mu-d} = 206(29)$, $\lambda^{(2)}_{dt\mu-d} = 450(50)$ and $\lambda^{(1)}_{dt\mu-t} = 23(6)$ in units of $10^6 s^{-1}$ at temperatures below 130K.

Recent experiments involving X-ray/neutron measurements on DT μCF in high-density and high-C_t DT mixture at RIKEN-RAL have also produced, in addition to μ a sticking phenomena, important new insights concerning the formation mechanism of dtμ. The results can be summarised as follows.

- The density dependence, which had been observed from the gas phase to the liquid phase (ϕ=1.2), seems to exist from liquid to solid (ϕ = 1.5) in C_t = 0.28 and 0.70, suggesting that the three-body collision effect in $\lambda_{dt\mu}$ does coexist under the condensed-matter effect.
- The ^{3}He accumulation effect, really significant in the solid but not significant in the liquid, has been precisely measured in order to be used for an interpretation of $\lambda_{dt\mu}$.

As for the well-understood DD μCF, it was found that there is a marked deviation between the experiment and theory below 20K, corresponding to the solid phase (Demin 1995, Knowles 1995). The deviation should be explained by the following two mechanisms (either one of two or both of them): a) due to a non-thermalisation effect during the slowing-down of (dμ), the existence of an energy gap in solid D_2 does suppress complete slowing-down, thus producing a non-thermalised epithermal (dμ) (about energy being 20K); b) the resection mechanism of the molecular formation may be dramatically changed due to a change in the final-state energy spectrum .

2.2 Future of muon catalysed fusion

Possible applications of the μCF have been considered in various fields. At this moment, the following three subjects are under serious discussions towards realization; a) an energy source; b) a 14-MeV neutron source and c) an ultra-slow μ^- source. Let us consider the first subject, namely, related to the energy problem.

Energy production of muon catalysed fusion

In order to consider the energy-production efficiency, it is required to know how much energy is needed to produce a single muon (a muon cost). There have been several discussions on the optimization of π^- production and $\pi^- \rightarrow \mu^-$ conversion. For π^- production, the fundamental processes in the nucleon-nucleon inelastic process are nn $\rightarrow$ p$\pi\pi^-$ and nπ $\rightarrow$ppπ^-. Therefore, the use of accelerated nuclei other than protons is inevitable. A deuteron beam as well as a triton beam have been considered for a cost (energy) estimation for economical μ^- production.

Following the argument made by Petrov et. al. (1979), a realistic solution seems to be as follows. By using a 1GeV/nucleon t(d) beam bombarded onto Li or Be nuclei, we can obtain 0.22(0.17) π^- from a single t(d). By using a large- scale superconducting solenoid with a reflecting mirror, one can expect 75 % efficiency for μ^- production from a single π^-. Thus, a 1GeV energy of t(d) produce 0.17 μ^- so that one μ^- can be produced by an energy of 6(8) GeV. Sometimes, by selecting the values mentioned for π^- production in a t-t collision the eventual cheapest cost would be about π^-/4GeV and μ^-/5GeV.

Several ideas have been proposed how to reduce the muon cost. Studies have been done for optimizing the type of incident accelerated particle, particle energy and choice of the fixed target. By summarizing these studies, the optimization does not seem to exceed the value mentioned above (π^-/4GeV). Another method to reduce the π^- production cost is to use a colliding beam. In this case, the energy of the center-of-mass motion, which is wasted at a fixed target geometry, would be efficiently used. It is claimed that π^-/1.8GeV (0.55 π^-/GeV) can be realised by a d-d collider. However, the realization of a beyond-MW-MW collider is totally uncertain.

On the other hand, the energy-production capability $E^{\rm out}_{\mu CF}$ of the μCF is determined by $E^{\rm out}_{\mu CF}$= 17.6× Y_n (MeV) in the case of DT μCF, which has a stringent limiting factor due to the sticking probability ω_s like $E^{\rm out}_{\mu CF} \leq 17.6\times\omega_s^{-1}$ (MeV). A situation related to $E^{\rm out}_{\mu CF}$ is summarised in Figure 10.

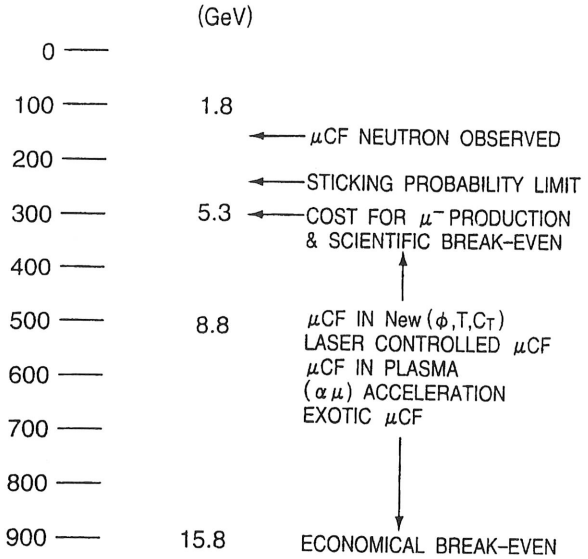

Figure 10. *Number of fusions and produced energy from dtm-μCF with required remarks.*

Several remarks can be given for a possible increase in the energy- production capability from the DT μCF. (a) Since the conditions so far used for the DT target in the μCF experiment, namely, density, temperature and C_t as well as the energy of the (tμ) atoms $E_{t\mu}$ controlled by the mixture of H_2 into DT mixture have not been satisfactory, there might exist more favorable conditions toward higher energy production; the μCF experiment at a higher density DT mixture, like $\phi = 2\phi_0$, should be the typical example. (b) In

order to increase $\lambda_{dt\mu}$, more a favorable matching condition in terms of resonant molecular formation might exist which will be realised by exciting the molecular levels of D_2 or DT by e.g. lasers. (c) In order to decrease ω_s, or in order to in crease R, several ideas have been proposed, and, among them, the use of a DT plasma where enhanced regeneration is expected due to an elongated $(\alpha\mu)^+$ mean-free path as well as the application of electric field acceleration of $(\mu\alpha)^+$ might be worth trying (d) In an actual 10–100MW power plant, if it exists, there might be several μ^- associated atoms or molecules interacting with each other, and thus causing a new non-linear phenomena possibly associated with a higher energy production which should be examined by using a high-brightness muon beam, like slow μ^-.

Contrary to the energy-production-India solely via the μCF, the concept of muon catalysed hybrid reactor has been proposed by Petrov (1980) and later by Eliezer *et al.* (1987). There, the accelerated 1-GeV/nucleon d beam is bombarded on Li or Be target with the remaining beam stopping in ^{238}U, where ~30% of the beam is spent on π^- production and 70% is spent on ^{238}U fission and ^{238}Pu production as electronuclear breeding. The produced π^- is used for the μCF in DT mixture, where produced 14-MeV neutron stops in the blanket of ^{238}U and ^{6}Li producing ^{239}Pu and T. The Pu thus produced is used for thermal nuclear reactor and the fission energy is used to feed the accelerator and the rest of the system. It is concluded that the proposed hybrid system can double the electric-power output of non-hybrid electronuclear breeding. There is an argument against the use of the μCF for fuel production of a thermal nuclear reactor which brings all the problems of a nuclear reactor like radioactive waste disposal, etc.

14-MeV neutron source

When thermal nuclear fusion becomes realistic, it is pointed out to be important to develop a material to be used for the first wall next to the inner-most core of the fusion reactor. For this purpose, it is important to investigate a highly irradiation test facility by 14-MeV neutrons. One practical idea is to have an intense source of a 200keV d beam and produce 14-MeV neutrons via the d + t $\rightarrow$ α + n reaction. In parallel to this idea, the 14-MeV neutrons from the μCF can be considered to be an alternative way for the materials irradiation facility.

Some realistic scheme has been considered (Petitjean 1993). Let us consider 1.5GeV and 12mA deuteron accelerators available. By placing a 30–50cm graphite target under the confinement field of 5–10T superconducting solenoid, intense pion production and efficient μ^- production can be realised. There, the μCF in the DT target occur, followed by intense 14MeV neutrons on the order of 10^{14}/cm^{2}s for the material under testing placed at one surface of the DT container. Most importantly, the power consumption by the μCF method is substantially lower compared to that in the d accelerator method ($\approx$0.1!). An alternative idea has been proposed by Petrov. Some realistic plant design is in progress.

Slow μ^-

For the case of negative muons (μ^-), it has been considered to be very difficult to produce an intense slow μ^- beam due to the following reasons: (1) because of a strong absorption of stopped π^- inside matter, the $\pi^- \rightarrow \mu^-$ decay cannot be realised inside the target

material, so that there is no surface μ^-, except for a small probability for liquid H_2 or He; (2) because of muonic atom formation, the stopped μ^- cannot be liberated from the stopping material after thermalisation inside the condensed matter, and, thus, no re-emission can be expected for the case of μ^-.

For a more realistic estimate, the kinetics in μCF must be taken into account. In order to overcome the second difficulty, a new idea has been proposed for the source of slow μ^-, which will be realised with the help of μCF phenomena (Nagamine 1989). The principle is as follows (see Figure 11): (a) at the disappearance of the core nuclei of 5He at the instant of μCF, a slow μ^- with an energy of around 10keV is released; (b) this liberation process is known to be repeated up to 150 times during the μ^- lifetime; (c) after successive liberation processes of slow μ^-, we can expect that a significant fraction of the μ^- stopping inside a thin solid DT layer would be re-emitted from the surface.

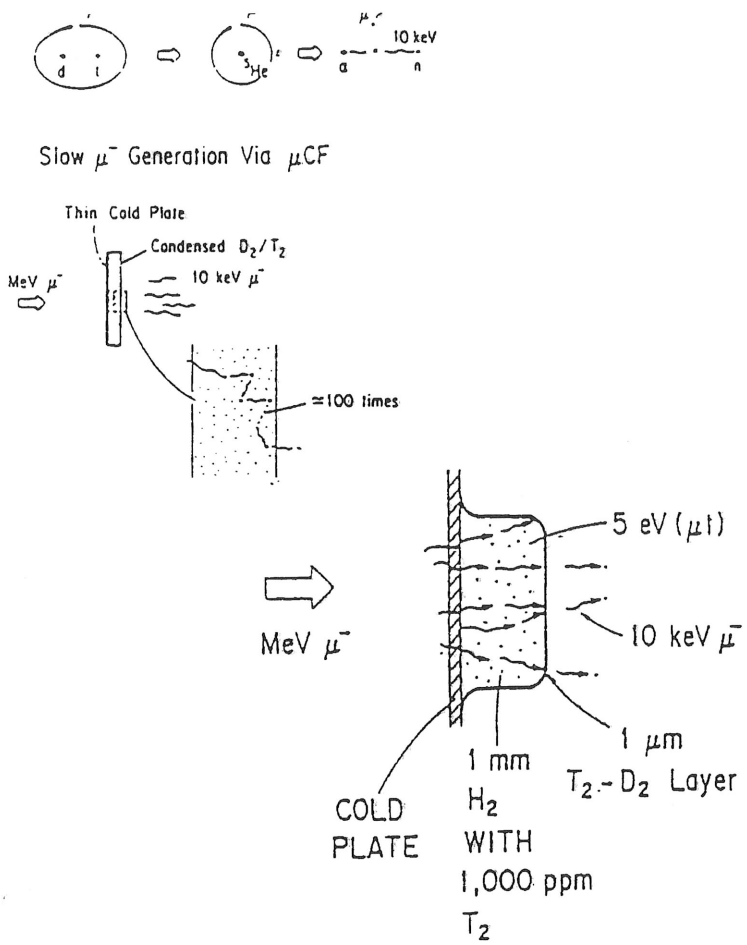

Figure 11. *Schematic view of low-energy m- production from dtm-μCF in a thin solid layer of a DT mixture and its extended version with a Ramsauer-effect enhancement.*

When there are no leakage processes from the DT layer, (solid and C_t being around 0.3–0.5) the conversion efficiency can be estimated to be the ratio of the range of the 10keV μ^- (0.3μm) versus that of the incoming μ^- with an energy of, say, 1MeV (0.9mm). The multiplication factor due to the number of μCF cycles is about$\sqrt{150}$, this giving $\sqrt{150}\times$ $0.3 \times 10^{-3}/0.9 = 0.004$. More realistically, the kinetics in μCF must be taken into account. For instance, the diffusion length of the neutral (dμ) or (tμ) gives a significant correction to the value mentioned above. Assuming 1μm for the diffusion length of (dμ) and (tμ) in the DT layer with a 7μm layer thickness, the conversion efficiency from stopping 1MeV a μ^- (below 10keV) emissions is around 2 $\times 10^{-4}$ instead of 4×10^{-3}.

In order to enhance the conversion efficiency, a two-layer structure was proposed by Marshall which would form an optimised DT layer on a 1mm thick H_2 layer with 0.1% T_2 (see Figure 11), the range of the injected MeV μ^- can be effectively reduced due to the Ramsauer-Townsend effect. Already, in order to confirm the reduced range concept, test experiments have been carried out at UTMSL/KEK and at TRIUMF for DD μCF by using 2eV (dμ) from the $H_2(D_2)$ mixture. There, a value of 1.5μm was obtained. Assuming that eV(tμ) stopping in the D_2 layer is similar to eV(tμ) stopping in the DT layer, one can obtain the conversion efficiency from 1MeV μ^- to the slow μ^- in a two-layer configuration, like 2×10^{-4} [0.9mm/1.5μm]$\times\epsilon_{t\mu} = 0.12\epsilon_{t\mu}$, where $\epsilon_{t\mu}$ is the emission probability of eV(tμ) from stopping μ^-. From our knowledge, $\epsilon_{t\mu}$ is around 0.1, leading to a conversion efficiency of 0.012.

The generation of intense slow μ^- has an important application field, namely, $\mu^+\mu^-$ colliders; for the TeV lepton colliders, a circular accelerating and colliding machine is only possible for muons having a limited synchrotron radiation loss. A slow muon source, as already realised for the μ^+ along with the slow μ^- source described here, can be efficiently used for a realistic cooling method of muons.

3 Muon life science

3.1 Introduction

As described in the other sections, the μSR method has been widely applied to explore new physics and chemistry in various condensed matter systems. According to some excellent features of the μSR method such as high sensitivity to the dynamical motion of the weak microscopic magnetism, it has for some time been suggested that the μSR can contribute to the solution of various bio-medical problems. Rather recently, namely since November 1997, some successful experiments have been performed to explore the microscopic nature of electron transfer in protein.

Under the name of muon life science, historically, the use of muonic X-ray is suggested to investigate the biological functions of human body through its capability of non-destructive element analysis of the specific organ in human body. Recently, a large-scale extension has been suggested by employing an ingenious photon-collimation system called a Sudare collimator to specify very accurately muon stopping region.

3.2 μSR application to bio-medical studies

Electron transfer in proteins

Electron transfer in macro-molecules such as protein is the most important mechanism for various biological phenomena such as storage and consumption of energy, photo-synthesis, brain function, etc.. Various experimental investigations have been applied to explore the electron transfer phenomena in protein related chemical compounds. One of the important methods to date to measure a long-distance electron transfer is to measure the electron-transfer kinetics from the reduced heme (Fe^{2+}) to the oxidised surface-bound Ru complex (Ru^{3+}) using a flash-quench procedure, thus concentrating on the specific path of the electron transfer. However, almost all the existing information on the electron transfer have been obtained by essentially macroscopic methods. It is quite important to study microscopically the electron transfer phenomena in proteins.

Among various types of proteins, cytochrome c attracts much attention (Pettigrew and Moor 1987, Scott and Mauk 1995), since it plays an essential role in the respiratory electron transport chain in mitochondria holding a position next to the final process of the cycle and transfers electrons to the surrounding oxidase complex. The three-dimensional molecular structure of cytochrome c has been determined by X-ray structural analysis in sixties.

Role of μ for electron-transfer studies

In order to obtain microscopic information on the electron transfer in the macro-molecule, the use of muon spin relaxation (μSR) method is potentially important. Polarised positive muons (μ^+), obtained in the MeV energy region from a beam channel installed at a high energy proton accelerator facility, can be injected into a biological substance (Figure 12a). During the slowing-down process, the injected μ^+ picks up one electron to form a neutral atomic state called muonium (Figure 12b). The muonium is then thermalised followed by chemical bonding to a molecule of the substance. Then, depending upon the nature of the molecule, the electron brought by the μ^+ into the molecule can take a characteristic behaviour including localization to form a radical state or a linear motion along the chain (Figure 12c). These behaviours can be detected most sensitively by measuring the spin relaxation process of the μ^+ using the μSR method. Muon spin relaxation occurs through a magnetic interaction between the μ^+ and the moving electron produced by the μ^+ itself. Here, the μ^+ takes a double role, namely, an electron producer and a sensitive observer of the electron behaviour.

This idea of the sensitive detection of the electron behaviour in macro-molecules has been successfully applied to the studies of electron transport in conducting polymers. A soliton-like motion in trans-polyacetylene, in contrast to the localization in the formation of a radical state in cis-polyacetylene, has been studied for the μ^+ produced electron (Nagamine 1984, Ishida 1985). Polaron-type electron transport phenomena in poly-aniline has also been studied (Pratt 1997).

Some significant observables in the μSR studies can be summarised as follows. In longitudinal relaxation measurements, due to the dipolar interaction between moving electrons and stationary muons, the characteristic dimensionality of the electron motion

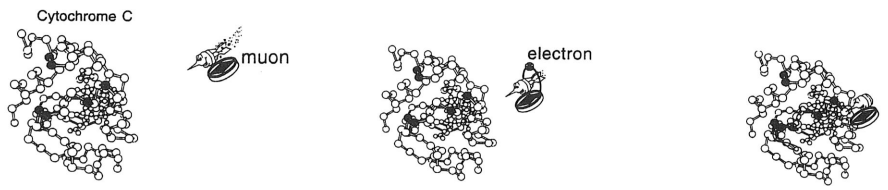

Figure 12. *Behaviour of μ^+ after being injected in to macro-molecules: (a)high energy μ^+ injection; (b) slowing-down and electron capture to form muonium (μ^+e^-) followed by deceleration of the muonium; (c) chemical bonding of the muonium and electron emission followed by electron localization or motion along the molecular- chain.*

can be studied by the external field ($B_{\rm ext}$) dependence of the muon spin relaxation rate (λ_μ) ; for the one-dimensional electron motion $\lambda_\mu \propto [B_{\rm ext}]^{-1/2}$, for the two-dimensional electron motion $\lambda_\mu \propto [\log B_{\rm ext}]^{-1}$ and for the three-dimensional electron motion λ_μ does not have $B_{\rm ext}$ dependence (Butler 1976).

Progress has been made toward the theoretical understanding of this paramagnetic relaxation process by considering the direct stochastic treatment of the random-walk process of a spin which is rapidly diffusing along a topologically one-dimensional chain (Risch and Kehr 1992). An error-function type longitudinal relaxation function (called R-K function, hearafter) $G(t) = \exp(\Gamma t)\,\mathrm{erfc}\,(\sqrt{\Gamma t})$ was proposed for $\lambda t_{\rm max} \gg 1$, where λ is the electron spin flip rate, $t_{\rm max}$ is the experimental time scale and Γ a relaxation parameter. In recent experiments, the usefulness of the R-K function has been confirmed experimentally for the polaron-motion of conducting electrons in polyaniline. In this theoretical treatment, Γ is proportional to $1/B_{\rm ext}$ in the case of a linear electron motion.

As a natural extension of this type of application of the μSR method, possible studies of electron transfer in protein have been proposed in 1987 by the present author (Nagamine 1987). None of the μSR studies on protein have been made up to now.

μSR experiment on cytochrome c

Experiments on the μ^+ relaxation in cytochrome c have been conducted by using intense pulsed (a single pulse of 70ns pulse width and 20ms seperation under a pulse-kicker operation in the muon beam channel) 4MeV μ^+ at the RIKEN-RAL muon facility. By installing a large solid-angle μSR spectrometer, a precise and long-time range spin relaxation of the μ^+ can be measured in a relatively short measurement time (10^6 events/min). As established in earlier works of muon science experiments, the use of pulsed muons is essential for measuring long relaxation times appearing in the present type of spin relaxation studies.

The cytochrome c used here is a polycrystalline powder form extracted from horse heart (Wako-Chemical product). The present μ^+SR measurements at various temperatures (5–300K) under various longitudinal fields (0.0–0.4T) have been conducted by using the powder sample as received.

At each of the measurement temperatures, the μ^+ relaxation function which corresponds to a time-dependent change of the μ^+ polarization was found to have an external field dependence as depicted in Figure 13 for some typical temperatures and applied longitudinal fields. The observed relaxation functions, $G(t)$, were fitted by the R-K function

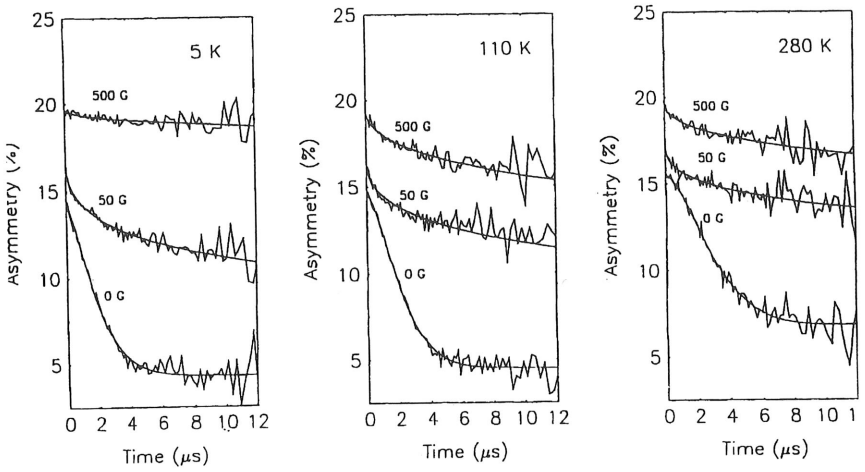

Figure 13. *Typical μ^+ spin depolarization time spectra in cytochrome at 5K, 110K and 280K under external longitudinal fields of 0G, 50G and 500G, where lines are fitting curves by using the R-K function.*

and the obtained longitudinal relaxation parameter Γ at various temperatures decreases monotonically against an increase of external field B_{ext} applied along the μ^+ initial spin direction (Figure 14), while initial asymmetry at $t = 0$, $A_\mu(0)$ increases against B_{ext}. (Note that the time dependent change of the spin polarization is described by $A_\mu(0)G(t)$). By a close look at the B_{ext} dependence of Γ, there seems to be two components: (1) a weak-field dependence region (lower field) and (2) a $(B_{\text{ext}})^{-1}$ dependence region (higher field). The latter region seems to exhibit the characteristic μ^+ spin relaxation due to a linear motion of a paramagnetic electron. As seen in Figure 14, the critical field (hereafter, we call cutoff field) where the second region becomes significant over the first region has a temperature dependence; a lower cross-over field at lower temperature. As summarised in Figure 15, temperature dependence of the cutoff field can be presented as having two components; one with an activation energy of 150meV (dominant above 200K) and the other with that less than 2meV (dominant below 200K).

Over the entire temperature range the initial amplitude $A_\mu(0)$ recovers with increasing weak-field. It shows, a first recovery at lower field (up to 300G) and then it shows a second recovery at higher field (above 300G) (see Figure 14). The low-field recovery along with the weak-field dependence of Γindicates that μ^+ depolarization takes place due to the dynamics of the surrounding molecules, while the high-field recovery along with $(B_{\text{ext}})^{-1}$ dependence of Γ reminds us that the μ^+ depolarization is due to the effect of a linearly moving electrons.

Revealed microscopic aspects of electron transfer in cytochrome c

All of these results may support the following microscopic pictures of the electron transfer process in cytochrome c.

1. An electron brought in by the μ^+ and liberated at the bonding site makes a topo-

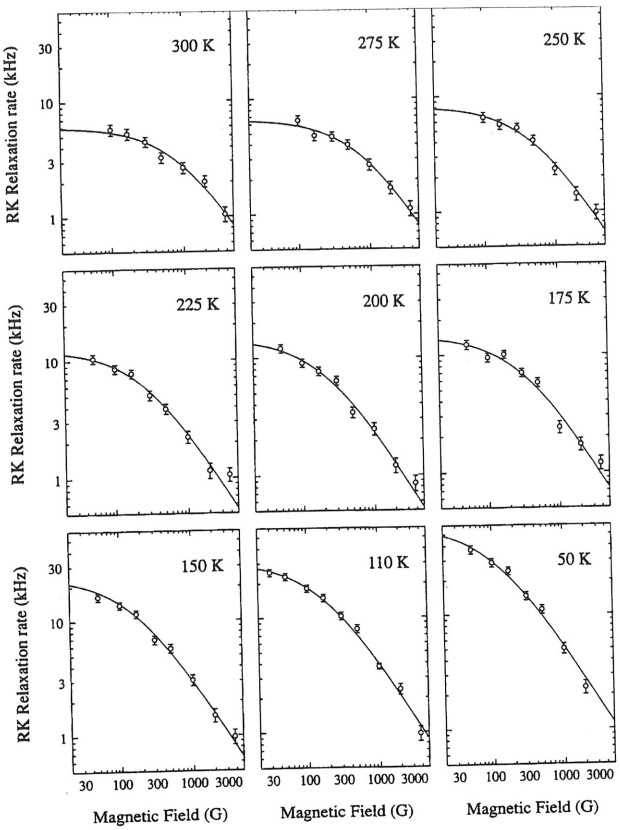

Figure 14. *The relaxation parameter versus external longitudinal magnetic field for the μ^+ in cytochrome c at various temperatures, where the B^{-1} dependence part can be seen to become significant at higher field region and the critical field (cutoff field) of the onset of the B^{-1} dependence can be seen to have a clear temperature dependence.*

logically linear motion along the chain of the cyctochrome c.

2. The electron transfer process, depending upon the temperature region, has two different modes as seen in the temperature dependence of the cutoff field (Figure 15) ; one with a characteristic activation energy of 150meV seen above 200K and the other with an activation energy of less than 2meV seen below 200K. The characteristic change at 200K of the cutoff field seems to be related to the well-known structure change of some proteins which has suggested as glass-like transition. A naive picture based upon previous μ^+SR studies on conducting polymers suggests an increase of a three-dimensional diffusion at temperatures higher than 200K. It is not clear whether this picture is consistent with a glass transition or not.

3. The diffusion rate along the chain D_L, which can be obtained by the measured Γ and the hyperfine coupling constant (500MHz) estimated from the recovery curve of the initial asymmetry, becomes a value of the order of 10^{12}rad/s and almost temperature-independent (Figure 15). The obtained D_L can be converted to the

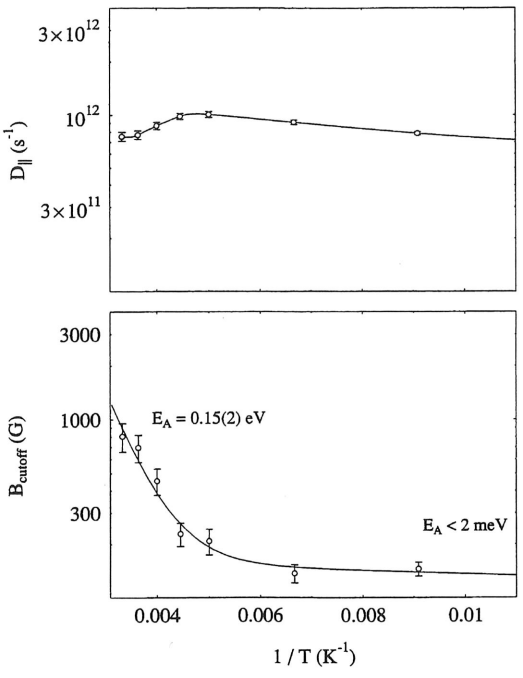

Figure 15. *The cutoff field determined in Fig.2 against inverse temperature, where activation-type energies can be determined (below). The temperature dependence of the diffusion constant of electron(s) in cytochrome c derived from the B^{-1} dependent part of the relaxation parameter (above).*

velocity v_e of 10m/s assuming $D_L = v_e l$ where l is the mean free path and taken as a size of cytochrome c (100Å) .

The most important remaining problems in the present μ^+SR studies might be: (1) Where is the location and electronic structure of the μ^+? (2) From where the electron takes a linear motion? At this stage of our μSR studies, there is no information on these questions. In this respect, the lower field relaxation part seen in Γ for $B_{\rm ext}$ below the cross-over might provide key information; if it comes from the magnetism of the Fe ions situated at the center of cytrochrome c, by measuring a precise value of the hyperfine interaction parameter between the stationary μ^+ and the Fe ion (and its temperature as well as angular dependence) may reveal the μ^+ location. For this purpose, muon spin rf resonance as well as level crossing resonance will be most helpful and be conducted in the nearest future.

Although, as mentioned above, there are some unknown factors in the nature of the μ^+ probe, the electron transfer phenomena through the microscopic section of somewhere in cythochrome c was directly detected in the present experiment. The present μSR method should be compared to the experiments using photo-excited electrons, where electron transfer was measured through a path connecting between heme-Fe and Ru-substituted portion (bis (2,2′-bipyridine) imidozale). It should also be compared to the

electron transfer measurements within a zinc-substituted protein initiated by flash photoproduction, where electron transfer through a path connecting heme-centres is inhibited.

The μ^+SR measurement, where high efficiency of the measurements should be emphasised (typically 5min. for each μSR spectrum shown in Figure 12, is easily able to be extended to cytochrome c in various chemical and biological environments; e.g. in solutions with different values of pH, etc. It is interesting to conduct similar experiments on other related proteins, such as (1) as suggested by N. Go, (Lysozyme without Fe ions where no electron transfer is expected) and (2) as suggested by Ataka and Kubota, cytochrome c with Fe^{2+} ions where electron transfer is somewhat suppressed. Preliminary measurements on these systems have given some supporting evidence, details of which will be reported elsewhere.

The highly sensitive μSR method which was successfully applied for the first time to prove a microscopic nature of the electron transfer phenomena in protein may open a wide-variety of application fields. Most importantly, because of the original high energy nature of the probe, this method can be applied to the protein in vivo. New information might be obtained on the basic functions of brain activity, for example.

3.3 Muonic X-ray studies of element analysis

As shown in Section 1, X-ray from the muonic atom formed by the injected μ^- and the atomic nuclei of the stopping material is a characteristic high-energy photon and can be easily detected by the detector placed outside the stopping substance like human body. The unique correspondence exists between Z of the stopping element and energy of muonic X-ray e.g. K_α X-ray line in the 2p$\rightarrow$1s transition as seen in Figure 16.

At the same time, stopping region of the μ^- can be determined by the range-energy direction in the depth (x) direction and by beam-collimation and/or beam positional-identification in the (xy) distribution along the plane perpendicular to the beam. Each distribution has a spacial broadening-width according to a range straggling as well as a momentum width of the beam in z-direction and a range straggling as well as a multiple-scattering in xy direction. A realistic case, namely for the μ^- with a momentum spread of 5%, is shown in Figure 17. Again, for 100MeV/c corresponding to the range in water of 10cm, both longitudinal and transverse spreads become 3.0mm.

As described in Section 1, the rate of muonic atom formation is roughly proportional to the product of Z-value of the element and elemental concentration $C(Z)$. Therefore, for the qualitative purpose at least, the intensity of the muonic X-ray after correcting energy-dependent efficiency one can obtain elemental concentration $C(Z)$ in the local region, where the μ^- is stopping.

Element analysis by the muonic X-ray method can be carried out using an experimental set-up schematically shown in Figure 18, where beam collimator as well as a range-adjusting energy-absorber is placed to control the stopping region of the μ^-.

A typical example of the muonic X-ray analysis to medical diagnostics is in the case of osteoporosis which is known to be a disease due to the anomalous Al concentration in the central trabecularpart of the human backbone. As is seen in Figure 19, depth-profile of the Al concentration has been measured for a model called phontom by Tohoku-Tokyo collaboration experiment conducted at TRIUMF (Sakamoto 1992).

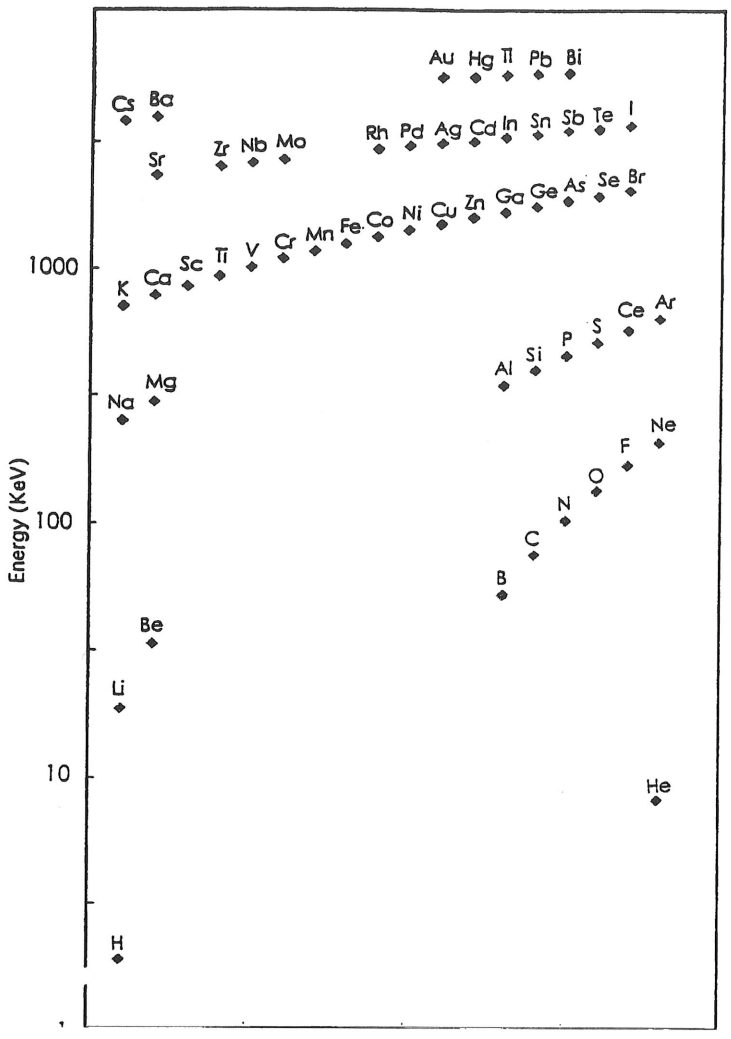

Figure 16. *Typical energies of muonic K_α X-ray.*

Recently, a new advanced method of muonic X-ray element analysis was proposed by employing Sudare collimator invented by M. Oda which has applied to various astrophysical problems. It employs essentially a photon-collimation by the detector-slit to identify a narrow line connecting from the photon source of the μ^- stopping location to the narrow area of the detector.

By using the Sudare collimator, it is expected to achieve spacial resolution better than 0.1mm for the plane perpendicular to the line toward the photon detector (Oda 1996). With a sub-mm spacial resolution, element analysis in vivo may reveal an important function of the human body to probe a movement of the dilute imparity like oxygen increase in hemoglobin related to the brain function.

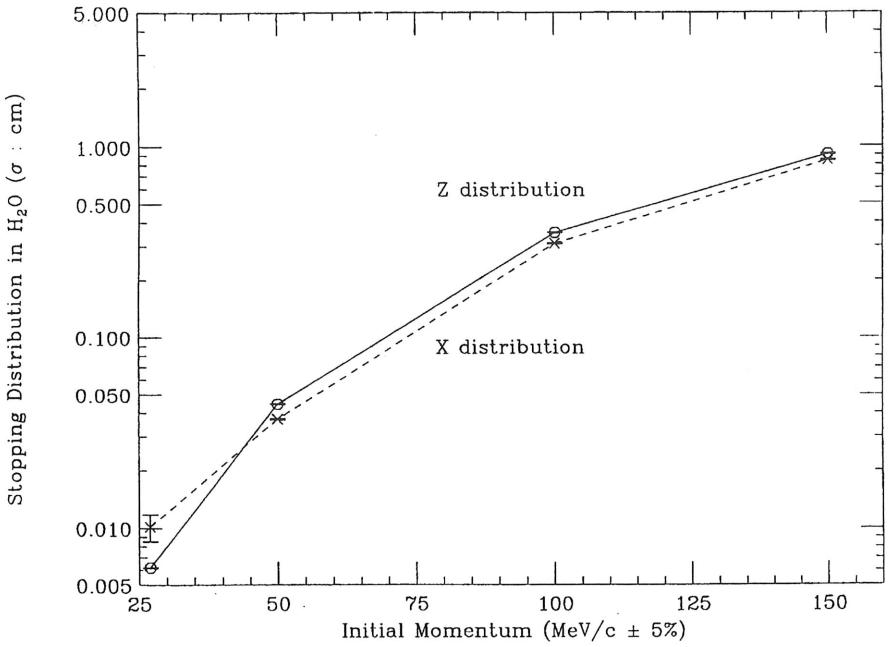

Figure 17. *Spacial distribution of the m- injected into water.*

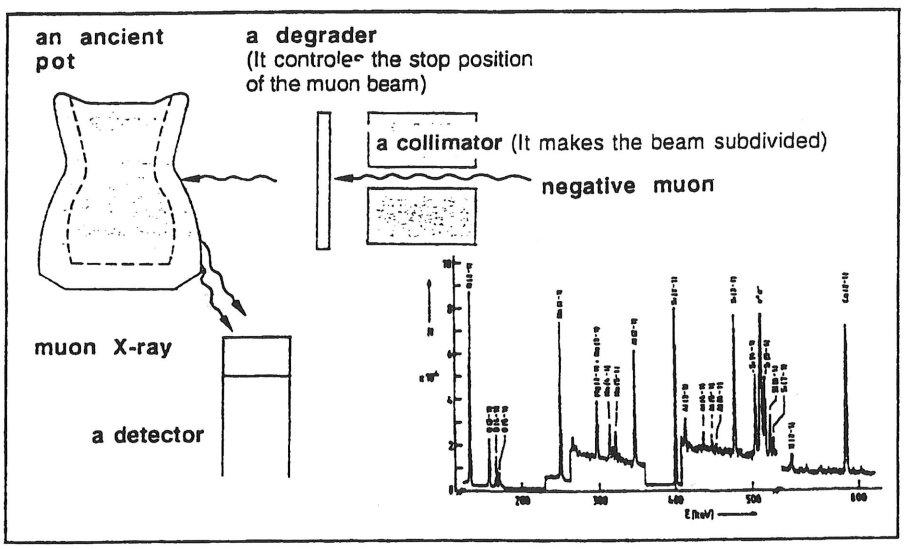

Figure 18. *Experimental arrangement of muonic X-ray element analysis.*

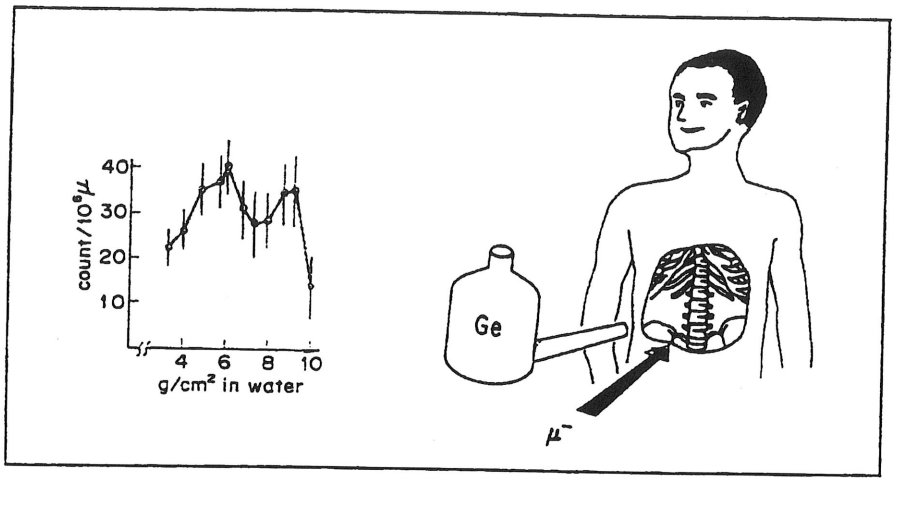

Figure 19. *Schematic view of osteoporosis diagnostics by using muonic X-ray method with experimental result on the phontom.*

References

Alvarez L W *et al.* 1957, *Phys Rev* **105**, 1127.

Bogdanova L N, *et al.* 1988, *Muon Catalysed Fusion.* **3**, 359..

Bogdanova L N, 1982, 1990/1991, *Sov Physics, JETP,* **56**, 931.

Bossy H *et al.* 1987, *Physical Review Letters*, **59**, 2864.

Breunlich W H, Kammel P, Cohen J S and Leon M, 1989, *Ann Rev Nucl Sci* **39**, 311.

Brunlich W H *et al.* 1987, *Physical Review Letters*, **58**, 329.

Butler M A, Walker L R and Soos Z G, 1976, Dimensionality of spin fluctuations in highly anisotropic TCNQ salts, Journal of Chemical Physics **64**, 3592–3601.

Daniel H, 1975, *Phys Rev Lett* **35**, 1649.

Demin D L *et al.* 1996, *Hyperfine Interacions*, **101/102**, 13.

Elieger S *et al.* 1987, *Nuclear Physics*, **127**, 527.

Fermi E and Teller E, 1947,*Phys Rev* **72**, 399.

Frank F C, 1947, *Nature* **160**, 525.

Froelich P *et al.* 1995, *Physical Review Letters*, **75**, 2108.

Gerstein S S and Ponomarev L I, 1977, *Physical Letters*, **728**, 80.

Nagamine K, 1987, Invited Talk at Gordon Conference on Rapid Electron Transfer in Macro-Molecule (Los Angels, March)

Ishida K, Nagamine K, Matsuzaki T, Kuno Y, Yamazaki T, Torikai E, Shirakawa H, and Brewer J H, 1985, Diffusion properties of the muon-produced soliton in trans-polyacetylene. *Physics Review Letters* **55**, 2209–2212.

Jackson J D, 1957, *Physical Review Letters*, **106**, 330.

Jones S E, *et al.* 1983, *Physical Review Letters*, **52**, 1757.

Jones S E, *et al.* 1983, *Physical Review Letters*, **56**, 588.

Kamimura M, 1989, AIP Conference Proceeding, **181**, 330.

Knowles P E *et al.* 1996, *Hyperfine Interactions* **101/102**, 21.

Leon M and Seki R, 1977, *Nucl Phys* **A282**, 445.

Nagamine K, Ishida K, Matsuzaki T, Nishiyama, K, Kuno W, Yamazaki Y, and Shirakawa H, 1984, Solitons in polyacetylene produced and probed by positive muons. *Physics Review Letters* **53**, 1763–1766.

Nagamine K and Kamimura M, 1998, *Adv Nucl Phys*, **24**, 151.

Nagamine K *et al.* 1987, *Muon Catalysed Fusion* **1**, 137.

Nagamine K *et al.* 1990, *Muon Catalysed Fusion* **5**, 239.

Nagamine K *et al.* 1993, *Hyperfine Interactions*, **82**, 943.

Nagamine K, Proceedings Japan Academy.

Oda M, 1996, private communication.

Pettigrew G M, and Moor G R, 1987, Cytochrome c (Biological Aspects), Springer-Verlag, Berlin-Heidelberg-New York-London-Paris-Tokyo.

Petitjean C *et al.* 1993, PSI Report PSI-PR-93-09.

Petrov Y V *et al.* 1979, *Sov Journal Nuclear Physics*, **30**, 66.

Petrov Y V, 1980, *Nature*, **285**, 466.

Ponomarev L I, 1973, *Ann Rev Nucl Phys* **23**, 395.

Ponomarev L I, 1990, *Contemporary Phys* **31**, 219.

Pratt F L, Blundell S J, Hayes W, Nagamine K, Ishida K and Monkman A P, 1997, Anisostropic polaron motion in polyaniline studied by muon spin relaxation. *Physics Review Letters* **79**, 2855–2858.

Risch R and Kehr K W, 1992, Direct stochastic theory of muon spin relaxation in a model for trans-polyacetylene, *Physics Review Letters* **B46**, 5246–5257.

Sakamoto K, Hosoi Y andNagamine K, 1992, New diagnostic methods using muonic X-rays, Perspectives of Meson Science 487, edited by Yamazaki T, Nakai K and Nogami K (North Holland).

Sakharov A D, 1948, Report FIAN, 1.

Schneuwley H, 1977, Proceedings of Erice School on Exotic Atoms, eds. Fiorentini G *et al.* Pisa, 255.

Scott R A, and Mauk A G, 1995, Cytochrome c –a multidisciplinary approach, University Science Books, Sausalito, California.

Struensee M C *et al.* 1988, *Physical Review* **A37**, 340.

Szalewicz K *et al.* 1990/1991, *Muon Catalysed Fusion* **5/6**, 241.